



Published in final edited form as:

ACS Synth Biol. 2015 July 17; 4(7): 788–795. doi:10.1021/acssynbio.5b00040.

Rationally Designed MicroRNA-Based Genetic Classifiers Target Specific Neurons in the Brain

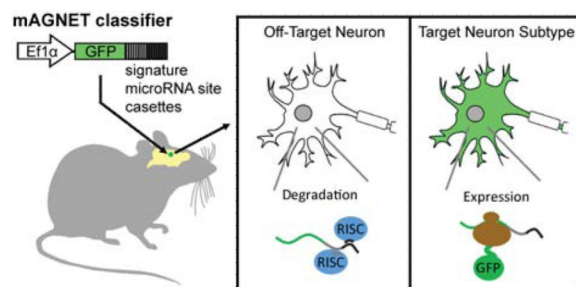
Marianna K. Sayeg[#], Benjamin H. Weinberg[#], Susie S. Cha, Michael Goodloe, Wilson W. Wong^{*}, and Xue Han^{*}

Department of Biomedical Engineering, Boston University, Boston, Massachusetts 02215, United States

[#] These authors contributed equally to this work.

Abstract

Targeting transgene expression to specific cell types *in vivo* has proven instrumental in characterizing the functional role of defined cell populations. Genetic classifiers, synthetic transgene constructs designed to restrict expression to particular classes of cells, commonly rely on transcriptional promoters to define cellular specificity. However, the large size of many natural promoters complicates their use in viral vectors, an important mode of transgene delivery in the brain and in human gene therapy. Here, we expanded upon an emerging classifier platform, orthogonal to promoter-based strategies, that exploits endogenous microRNA regulation to target gene expression. Such classifiers have been extensively explored in other tissues; however, their use in the nervous system has thus far been limited to targeting gene expression between neurons and supporting cells. Here, we tested the possibility of using combinatory microRNA regulation to specify gene targeting between neuronal subtypes, and successfully targeted inhibitory cells in the neocortex. These classifiers demonstrate the feasibility of designing a new generation of microRNA-based neuron-type- and brain-region-specific gene expression targeting neurotechnologies.



^{*}Corresponding Authors wilwong@bu.edu, xuehan@bu.edu..

Supporting Information

One table, three figures, and miRNA cassette sequence data. This material is available free of charge *via* the Internet at <http://pubs.acs.org>.

The authors declare no competing financial interest.

Keywords

synthetic biology; genetic classifier; microRNA; neuroengineering; gene therapy; inhibitory neurons

The ability to genetically modify specific cell types is essential in defining their contributions to physiological systems, such as the functional role of neural subsets in brain computation and behavior. Genetic classifiers are synthetic gene expression systems designed to restrict transgene expression to particular classes of cells, to facilitate cell-type characterization. Most commonly, they rely upon transcriptional promoters with tissue-restricted expression patterns to define cellular specificity. It has been challenging to develop genetic classifiers for use in the brain, due to the limitations of current gene delivery methods and difficulties identifying and recapitulating natural neuron-type specific promoters. While whole animal transgenic techniques have provided invaluable resources for targeting gene expression to specific cells, viral gene delivery remains an important technique to further expand the utility of transgenic models,¹ to target gene expression in genetically intractable species, and to advance human gene therapy. Viral techniques are particularly important in the brain because nonviral methods tend to be inefficient in transducing postmitotic cells such as neurons.

One major challenge facing viral gene delivery is the limited DNA packaging capacity characteristic of the most reliable and widely used gene therapy vectors, lentivirus and adeno-associated virus (AAV).^{2,3} Consequently, there are usually complications effectively packaging large cell-type-specific promoters in these viruses. Some shortened promoters have achieved remarkable specificity in lentiviral or AAV vectors;³⁻⁵ however, for many cell types it is difficult to identify a short promoter element with sufficient specificity.^{2,3} Viral pseudotyping has been explored as a supplemental means of increasing targeting specificity;^{6,7} however, envelope protein choices are limited, and modifications are often difficult to engineer while maintaining virus stability. Here we explored an alternative classifier platform, ideally suited for viral delivery, which exploits endogenous microRNA (miRNA) regulation to target gene expression to specific neuron subtypes in the living brain.

miRNAs are small (~20 nt), noncoding RNAs that inhibit gene expression by hybridizing to complementary recognition sites within mRNA transcripts, leading to repressed translation or direct degradation of their gene targets. A given miRNA tends to regulate sets of related genes, and its expression is usually correlated to that of its downstream targets.⁸ Genetic classifiers incorporating miRNA recognition sites have been demonstrated extensively in cell culture.^{9,10} Because miRNAs are inhibitory, miRNA-based classifiers function by blocking expression in off-target cells rather than positively driving expression in target cells, and thus it presents additional challenge to design such classifiers to exclude all off-target cell types for *in vivo* applications. Viral miRNA-based classifiers have started to emerge for select applications *in vivo*, including improving gene expression targeting in the liver and spleen,¹¹⁻¹³ and restricting stem cell therapies to the tumor microenvironment.^{11,14,15} Within the nervous system, micro-RNA-based classifiers have shown potential in restricting transgene expression to astrocytes¹⁶ or photoreceptors.¹⁷

Exploiting miRNA regulation to target gene expression is an attractive technique for brain research due to the small footprint of miRNA sites (which facilitates viral packaging), the potential to engineer combinations of miRNA sites to tune selectivity, and the possibility of targeting the many neuron types in the brain for which no cell type specific promoters have been identified.

In light of the recent characterization of neuron-type and brain-region specific miRNA profiles in mice,¹⁸ we hypothesized that miRNA-based classifiers could be rationally designed to specify gene targeting not only between neurons and supporting cells, but between neural subtypes. To explore this principle, we designed several virally deliverable, neuron-type specific, miRNA-based classifiers (for simplicity, miRNA-guided neuron tags: mAGNETs), and tested the combinatory effects of different miRNAs in targeting a known cell type, cortical inhibitory neurons. Because of the size and complexity of natural inhibitory-neuron-specific promoters, it has been difficult to engineer lentivirus or AAV to target these cells. Much effort has been directed toward targeting inhibitory neurons with shortened promoters,¹⁹ and a limited set of nonmammalian promoter sequences used in conjunction with AAV serotype targeting have shown promising selectivity.³ Here, we present a novel neuron subtype targeting strategy, orthogonal to promoter-based strategies, that exploits endogenous microRNA regulation to target gene expression. We were able to achieve inhibitory-neuron-specific targeting using signature miRNAs that selectively inhibit expression in excitatory cells and spare expression in the targeted inhibitory cells. The presented mAGNETs demonstrate the feasibility of rationally designing neuron-type-specific classifiers driven entirely by miRNA regulation, completely orthogonal to promoter- or serotype-based gene targeting strategies.

To test the feasibility of using miRNA regulation to target neural subtypes, we designed several mAGNET classifiers specific to cortical inhibitory neurons. Because miRNA regulation is inhibitory, we analyzed the cell-type and brain-region-specific miRNA expression profiles reported by He *et al.*¹⁸ seeking signature miRNAs strongly associated with excitatory neurons. We identified three signature miRNAs, miR-128, miR-221, and miR-222, which exhibited at least 1000 deep sequencing raw reads and had the greatest expression differences between excitatory and inhibitory neurons in the adult mouse cortex (see Table S1, Supporting Information). We then designed several mAGNET constructs containing cassettes of recognition sites for two or three of these signature miRNAs (see Figure 1a). The classifiers were built in lentiviral vectors containing a constitutive, nonspecific EF1 α promoter driving the expression of an EGFP reporter gene, with miRNA recognition cassettes positioned within the 3' UTR. We used an equivalent EGFP-only vector, without any miRNA recognition sites, as a control (see Figure 1a).

To test our classifiers in the brain, we produced high-titer lentiviruses of each mAGNET and the EGFP control, and injected them into adult mice at two locations in the cortex (Figure 1b, $n = 2$ mice for every construct under every testing condition). To quantify cell type preference resulting from either the EF1 α promoter or lentivirus tropism, we first analyzed EGFP expression patterns in mice injected with the control virus. We analyzed the colocalization patterns of EGFP + cells with an inhibitory neuron marker (GABA), an excitatory neuron marker (CamKII), and a glial cell marker (GFAP). In the cortex at 2

weeks postinjection, we found that approximately 13% of EGFP+ cells expressed GABA, 85% expressed CamKII, and 4% expressed GFAP (see Figure 1c and Table 1, 71 cells analyzed for GFAP staining). Note that immunohistochemistry for each marker was carried out on separate brain slices. These results confirm that our lentivirus with an EF1 α promoter infects primarily neurons (labeled only about 4% GFAP+ glia cells). Also, the observed 85% colocalization with CamKII is consistent with the distribution of excitatory to inhibitory neurons in the mouse cortex (approximately 80:20),²⁰ with a slight lentiviral infection bias toward excitatory cells.⁷

When we performed immunohistological analysis in mice infected with lentivirus-packaged mAGNETs, we noticed that EGFP+ cells were sparsely distributed within cortical injection sites compared to observations in EGFP control animals (see Figure 1d). The overall spread of EGFP+ cells appears similar in mice infected with the EGFP control or mAGNETs, suggesting that all viruses achieved identical efficiency in infecting cells, although mAGNET-labeled GFP+ cells are much more sparsely distributed. EGFP+ cells were clearly visible without any immunostaining and exhibit no observable difference in fluorescence intensity across mice, suggesting that the inclusion of miRNA recognition cassettes led to selective reduction of EGFP expression in some cells, but not all cells. Together, these results demonstrate that inclusion of multiple miRNA binding sites within mAGNETs did not interfere with lentivirus packaging, which is sensitive to repetitive DNA sequences, and that mAGNETs targeted EGFP fluorescence to a sparsely distributed population of neurons.

We next further examined the mAGNETs' targeting specificities between excitatory and inhibitory neurons. When designing our mAGNETs, we noted that the expression level of candidate signature miRNAs varied drastically. For example, the raw sequencing reads for miR-128 and miR-222 span 4 orders of magnitude (see Table S1), suggesting that they might differ in transgene inhibition efficiency. We designed the first two mAGNET constructs to test the expression threshold for consideration as a signature miRNA. The 4X2C mAGNET contains recognition cassettes for the two signature miRNAs with the highest raw reads, miR-128 and miR-221, whereas the 4X3C mAGNET contains cassettes for all three (see Figure 1a). At 2 weeks postinjection, we found that of the cortical EGFP+ cells transduced by either 4X mAGNET, ~70% expressed GABA, and ~24% expressed CamKII (see Figure 2a,b, Figure 3b and Table 1). This result suggests that miR-222 does not contribute to mAGNET-mediated EGFP knockdown, and thus the expression threshold for consideration as a signature miRNA in this case is greater than 7200 raw sequencing reads (Table S1). These results demonstrate that miRNA expression threshold is a critical consideration for such classifier designs. The absolute threshold for a given application should probably be determined on a case-by-case basis, as it relies upon the strength of the promoter used in the viral vector, the ratio of miRNA expression in the target and off-target cells, the number of miRNA recognition site repeats, as well as other translation regulation factors.

To analyze the temporal dynamics of classifier specificity, we examined cells transduced by both 4X mAGNETs at 4 weeks postinjection, and found that GABA and CamKII colocalization remained the same for both mAGNETs (~71% of EGFP+ cells were GABA+, 191 and 158 cells for the 4X2C and 4X3C mAGNET respectively) (see Figure 2 c,d)

compared to that observed at 2 weeks postinjection. This suggests again that miR-222 does not contribute to mAGNET-mediated EGFP knock down and that expression of the other signature miRNAs does not vary significantly over time. The temporal stability of mAGNET targeting suggests that these signature miRNAs may be associated with constitutive pathways in excitatory cells that require constant regulation. In fact, it was recently discovered that miR-128 is an essential regulator of neuronal excitability.²¹ With further improvements, another interesting use for the presented mAGNET classifiers would be to selectively target and characterize the fraction of CamKII cells without repression, as they may constitute a novel subset of excitatory cells with different excitability.

We next tried to improve inhibitory neuron targeting by increasing the number of recognition sites for the two efficacious miRNAs. We designed one mAGNET with eight identical recognition sites for both miR-128 and miR-221, and another with 12 identical recognition sites for miR-128 only (8X2C and 12X1C mAGNETs, Figure 1a). The 12X1C mAGNET-targeted EGFP expression exhibited 72–73% colocalization with GABA+ inhibitory neurons in the cortex (see Figures 2f, 3b and Table 1), nearly identical to that achieved with the 4X2C and 4X3C classifiers. The 8X2C mAGNET, on the other hand, exhibited an increased specificity toward cortical inhibitory neurons, presenting 80–83% colocalization with GABA (Figures 2e, 3b and Table 1). This level of specificity is considerable, given that inhibitory cells make up only 20% of cortical neurons and lentivirus has a slight infection bias toward excitatory cells.⁷ These results affirm that multiplying the sites for one miRNA has only a small effect on repression,²² and further suggest that the synergistic effects of several signature miRNAs can be tuned to improve specificity.

To further verify the identity of the inhibitory cell population targeted by the 8X2C mAGNET, we analyzed the colocalization of EGFP+ cells with α -parvalbumin (PV) and α -somatostatin (SST) (Figure S1), and found that 30% are PV + ($n = 57$ cells), and 51% are SST+ ($n = 54$ cells). Although identical expression levels of miR-128 and miR-221 in PV+ and SST+ neurons were reported,¹⁸ miRNA activity may differ among inhibitory cell types within different cortical depth or layers. This suggests that with optimization, it may be possible to target specific subtypes of inhibitory neurons with mAGNET classifiers, a task that has proven difficult with shortened promoters.³

Because our classifiers were designed based on cortical miRNA profiles, and miRNA expression has been shown to vary between brain regions,^{18,23} we further examined the targeting specificity at a site distant from the cortex. Each mouse also received an additional lentivirus injection in the hippocampus (see Figure 3a), where cell-type-specific miRNA profiles are yet to be determined. We found that of the hippocampal EGFP+ cells transduced by any of the mAGNETs, <20% are inhibitory neurons (GABA+) and >80% are excitatory neurons (CamKII+), identical to results achieved with the EGFP control construct (see Figures 3b–d, S2 and Table 1). This indicates that miR-128 and miR-222 are not differentially expressed at high enough levels to bias mAGNET expression in hippocampal neurons. Tan *et al.* recently demonstrated that miR-128 governs the expression of ion channels relevant for motor control, and is several fold more prevalent in the cortex than in the hippocampus.²¹ It is probable that the lower expression level of miR-128 in hippocampus as well as the additive knockdown by miR-222 is driving the cortex-specific

inhibitory neuron targeting observed here. For all mAGNETs, inhibitory neuron targeting preference was consistent at the two cortical testing locations and across mice (see Figure 3b and Table 1), and there was no significant targeting effect in the hippocampus (Pearson's chi-squared test, see Supporting Information), indicating that our classifiers achieved brain-region specific targeting.

Finally, to test the possibility that miRNA-based classifiers might sequester miRNAs away from endogenous targets and affect cell phenotype, we characterized electrophysiological properties of neuron cultures transfected with one of our mAGNETs. After confirming a 98% cotransfection rate with calcium phosphate ($n = 295$ neurons examined), we inferred the identities of neurons cotransfected with the 4X2C mAGNET and a CamKII_mRuby2 excitatory cell labeling construct (see Figure S3a) as follows: EGFP+ only cells are inhibitory neurons that do not express CamKII, mRuby2+ only cells are CamKII-expressing excitatory neurons with miRNA-mediated EGFP repression, and EGFP+/mRuby2+ cells are CamKII-expressing excitatory neurons without miRNA-mediated EGFP repression (Figure 4a). We then recorded membrane currents using patch clamp recordings from neurons cotransfected with 4X2C mAGNET and CamKII-mRuby2, and those cotransfected with EGFP control and CamKII-mRuby2 (Figure S3c,d). Current–voltage profiles (Figure 4b,c) from neurons with various expression profiles showed no significant differences, indicating that mAGNET-mediated EGFP knockdown by endogenous miRNAs does not cause a significant change in electrophysiological properties measured here. Notably, we found that 4X2C mAGNET achieved a cortical inhibitory neuron targeting specificity of only 25% *in vitro*, (Figure S3b), in sharp contrast to the ~71% achieved *in vivo* (Table 1). This discrepancy indicates that neurons in culture have drastically different miRNA expression profiles than neurons in the brain, which is not surprising considering the distinct chemical and mechanical properties of their environment in culture. Thus, while *in vitro* neuron cultures represent an attractive larger-scale screening platform, it is preferable to optimize mAGNETs directly *in vivo*.

While it is desirable to maintain stable transgene expression levels for cell-type targeting applications, for other applications, miRNA regulation could be exploited to dynamically regulate transgenes and monitor phenotype changes. For example, classifiers based on highly variable signature miRNAs have been useful for monitoring neural stem cell differentiation.²⁴ In adult neurons, tools for monitoring phenotype changes, such as expression patterns of the transcription factor c-fos and the synthetic promoter E-SARE,^{25,26} have been designed to broadly target cells with elevated activity patterns. Better understanding of the pathways regulated by individual miRNAs will enable forward-engineering of mAGNET classifiers, providing a novel toolset to dynamically monitor a wide range of specific phenotype changes in adult neurons.

Here we have demonstrated the feasibility of using mAGNET classifiers to target a specific desired subset of neurons in the living brain, cortical inhibitory neurons. mAGNETs represent a compact, tailorable genetic classifier platform for neuron-type and brain-region specific gene expression targeting. The primary advantage of this classifier platform is that small miRNA recognition sequences can be easily packaged and modularly combined on the same circuit to tailor specificity in viral vectors relevant for gene therapy in the brain. The

~82% targeting rate achieved using only two signature miRNAs demonstrates the potential of the mAGNET approach, although further optimization for greater specificity is desirable for many neuroscience applications. There are several avenues to continuing optimization, including altering the ratio and placement of miR-128 and miR-222 sites, and exploring alternative signature miRNAs and promoters. The strong, constitutive EF1 α promoter used here may be driving transcription at a faster rate than the gene regulation capability of the signature miRNAs. Using a weaker promoter such as a synapsin promoter may allow more efficient repression in excitatory cells. One constraint in designing mAGNETs is that they are an inverse (inhibitory) targeting system, so signature miRNAs must be specific to off-target cells. However, we have shown that it is possible to choose one signature miRNA with high expression across many cell types and a high ratio of expression in off-target to on-target cell population(s) (ex. miR-128), which could potential eliminate the need of laboriously selecting signature miRNAs for each off-target cell type. Alternatively, mAGNETs could be engineered to utilize positive miRNA control through incorporation into multicomponent inverter circuits.²⁷

As the regulatory functions of individual miRNAs are further explored and quantitative models of miRNA regulation improve,²⁸ such classifiers can be designed for many neuroscience applications. For example, mAGNETs would be useful for targeting other difficult cell types *in vivo* and in genetically intractable species, targeting optogenetic²⁹ neurotechnologies to precisely characterize novel cell types,^{30,31} and monitoring dynamic phenotype changes in adult neurons. Furthermore, miRNA-based targeting could be used in conjunction with traditional promoter or Cre Recombinase strategies to enhance targeting specificity and reduce off-target effects, as has been demonstrated in other tissues.¹³ Finally, as individual miRNAs are becoming increasingly linked to different neurological and psychiatric diseases,^{32,33} mAGNETs could prove an effective platform for targeting gene therapies to diseased neuron populations. While the mAGNETs reported here represent a simple proof-of-principle, elaboration and optimization of these neuron-type specific classifiers could have substantial implications for neuroscience research and the future of human gene therapy.

METHODS

mAGNET Vector Construction

miRNA recognition sites were designed as the exact reverse complement of the identified signature mouse miRNAs. The designed miRNA recognition cassettes were positioned after GFP in a pHR-lentiviral transfer plasmid backbone (<http://www.addgene.org/50839/>) driven by an EF-1 α promoter (<http://www.ncbi.nlm.nih.gov/nucore/HQ644134.1>). Single-stranded DNA oligonucleotides containing the miRNA sites were synthesized by IDT DNA, annealed, and cloned into the NotI sites within the backbone through standard molecular cloning procedures (for sequences see Supporting Information).

Lentivirus Production

Replication-incompetent lentivirus was packaged *via* triple transfections of pHR-4X2C_mAGNET, pHR-4X3C_mAGNET, pHR-8X2C_mAGNET or

pHR-12X1C_mAGNET lentiviral transfer plasmid (will be deposited to PubMed and Addgene), plasmid pMD2.G encoding for VSV-G pseudotyping coat protein (<http://www.addgene.org/12259/>), and pDelta 8.74 (<http://www.addgene.org/5682>) helper packaging plasmid, into HEK293FT cells (Life Technologies, R700-07) using TransIT-293 transfection reagent (Mirus Bio LLC, MIR 2700), and then purified through ultracentrifugation. Viral titer was estimated to be 10^9 particles/mL on the basis of established titrating correlations between *in vivo* observations and *in vitro* HEK293FT infection.

Stereotaxic Surgeries

All procedures were done in accordance with the National Institutes of Health Guide for Laboratory Animals and were approved by the Boston University Institutional Animal Care and Use and Biosafety Committees. We injected each virus at three locations in the adult mouse brain (two-month-old, female C57b6 wt mice): cortex1 (+1.000 mm ML, +1.800 mm AP, -1.250 mm DV), cortex2 (+1.000 mm ML, -1.500 mm AP, -0.900 mm DV) and hippocampus (+1.000 mm ML, -1.500 mm AP, -1.750 mm DV). Two mice were injected per condition ($n = 12$ mice total). One microliter of lentivirus was injected per site.

Immunohistochemistry

At two or 4 weeks postinjection, mice were sacrificed and perfused with 4% PFA. Brains were postfixed in 4% PFA for 2 h, flash froze in OCT, and then sectioned at $40 \mu\text{m}$. Brain slices were stained with markers for GABA (Sigma, A2052), CamKII (Santa Cruz Biotech, sc-13082), GFAP (Millipore, AB5541), PV (Swant, PV25) or SST (Abcam, ab8904), followed by Alexafluor-568 goat-antirabbit or goat-antichicken secondary antibody and ToPRO-3 nuclear dye (Life Technologies).

Confocal Imaging and Quantification

Confocal imaging was performed on an Olympus FV1000 scanning confocal microscope, using a 60X water immersion lens. Z-stacks were taken by imaging at $2 \mu\text{m}$ intervals throughout the slices. EGFP + cell bodies were identified by comparison with ToPRO-3 nuclear staining, then each identified EGFP+ cell was categorized as immunopositive or immunonegative for the antibody stain. Note that staining for each marker was performed on separate brain slices. We analyzed 1–4 nonoverlapping confocal stacks from each of 2–6 slices per injection site, per mouse. At least 50 EGFP+ cells were analyzed per condition (see Pearson's Chi Squared Test). All hippocampal images were taken of the CA1 cell layer.

Pearson's Chi Squared Test

The Pearson's chi squared test statistic with one degree of freedom (since cells examined are either excitatory or inhibitory) was calculated for each colocalization percentage (Table 1) by taking the difference between the observed number of counts for inhibitory/excitatory cells and the expected distribution of 20% inhibitory and 80% excitatory cells. A chi squared test of independence with one degree of freedom requires an expected frequency of at least 10 to produce reliable approximations, and since inhibitory cells make up approximately

20% of neurons in the cortex and hippocampus, 50 neurons in each test was determined to be the minimum sample size.

Cortical Neuron Culture Transfection and Electrophysiology

All experiments were approved by Boston University Institutional Animal Care and Use Committee. Cortical neurons were harvested from CD-1 mice on postnatal day 0 or 1 as described previously.³⁴ Neuron cultures were transfected on day 5 with a combination of pHR-CamKII_mRuby2 and either pHR-4X2C_mAGNET or pHR-EGFP_Control (1.5 μ g per construct) *via* calcium phosphate transfection. Whole-cell voltage clamp recordings were performed on postnatal day 7 or 8 ($n = 6-8$ neurons per condition) with a Multiclamp 700A amplifier (Molecular Devices, LLC) controlled with pClamp 10 software (Molecular Devices, LLC). Cultured neurons were bathed in extracellular solutions that contained (in mM): 140 NaCl, 3 KCl, 2.5 CaCl₂, 1.5 MgCl₂, 10 HEPES, 11 glucose; (pH, 7.4, 305 mOSM). Patch electrodes were pulled from thick-walled borosilicate glass capillaries with resistances of ~ 5 M Ω and filled with intracellular solution that contained (in mM): 130 K-gluconate, 2 NaCl, 7 KCl, 1 MgCl₂, 1 EGTA, 10 HEPES, 2 ATP-Mg, 0.3 GTP-Tris; the (pH, 7.4; 290mOSM). All experiments were performed at room temperature. Neuron culture cotransfection rates were determined by transfecting day 5 cortical neurons with a combination of pHR-EGFP_Control and pHR-EF1 α _mKate, and quantifying EGFP and mKate colocalization at 24 h.

Supplementary Material

Refer to Web version on PubMed Central for supplementary material.

ACKNOWLEDGMENTS

X.H. acknowledges funding from NIH Director's New Innovator award (1DP2NS082126), NINDS (1R01NS087950, 1R21NS078660, 1R01NS081716), NIMH (5R00MH085944), Pew Foundation, Alfred P. Sloan Foundation, Michael J. Fox Foundation, NARSAD, Boston University Biomedical Engineering Department, and Boston University Photonic Center. W.W. acknowledges funding from NIH Director's New Innovator award (1DP2CA186574). B.W. is funded by NSF GRFP. We thank members of the Han Lab for suggestions on the manuscript.

REFERENCES

1. Heffner CS, Herbert Pratt C, Babiuk RP, Sharma Y, Rockwood SF, Donahue LR, Eppig JT, Murray SA. Supporting conditional mouse mutagenesis with a comprehensive cre characterization resource. *Nat. Commun.* 2012; 3:1218. [PubMed: 23169059]
2. Han X. Optogenetics in the nonhuman primate. *Prog. Brain Res.* 2012; 196:215–233. [PubMed: 22341328]
3. Nathanson JL, Jappelli R, Scheeff ED, Manning G, Obata K, Brenner S, Callaway EM. Short promoters in viral vectors drive selective expression in mammalian inhibitory neurons, but do not restrict activity to specific inhibitory cell-types. *Front. Neural Circuits.* 2009; 3:19. [PubMed: 19949461]
4. Matsuzaki Y, Oue M, Hirai H. Generation of a neurodegenerative disease mouse model using lentiviral vectors carrying an enhanced synapsin I promoter. *J. Neurosci. Methods.* 2014; 223:133–143. [PubMed: 24361760]
5. Dittgen T, Nimmerjahn A, Komai S, Licznarski P, Waters J, Margrie TW, Helmchen F, Denk W, Brecht M, Osten P. Lentivirus-based genetic manipulations of cortical neurons and their optical and

- electrophysiological monitoring *in vivo*. Proc. Natl. Acad. Sci. U. S. A. 2004; 101:18206–18211. [PubMed: 15608064]
6. Burger C, Gorbatyuk OS, Velardo MJ, Peden CS, Williams P, Zolotukhin S, Reier PJ, Mandel RJ, Muzyczka N. Recombinant AAV viral vectors pseudotyped with viral capsids from serotypes 1, 2, and 5 display differential efficiency and cell tropism after delivery to different regions of the central nervous system. Mol. Ther. 2004; 10:302–317. [PubMed: 15294177]
 7. Nathanson JL, Yanagawa Y, Obata K, Callaway EM. Preferential labeling of inhibitory and excitatory cortical neurons by endogenous tropism of adeno-associated virus and lentivirus vectors. Neuroscience. 2009; 161:441–450. [PubMed: 19318117]
 8. Bartel DP. MicroRNAs: target recognition and regulatory functions. Cell. 2009; 136:215–233. [PubMed: 19167326]
 9. Xie Z, Wroblewska L, Prochazka L, Weiss R, Benenson Y. Multi-input RNAi-based logic circuit for identification of specific cancer cells. Science. 2011; 333:1307–1311. [PubMed: 21885784]
 10. Prochazka L, Angelici B, Haefliger B, Benenson Y. Highly modular bow-tie gene circuits with programmable dynamic behaviour. Nat. Commun. 2014; 5:4729. [PubMed: 25311543]
 11. Brown BD, Naldini L. Exploiting and antagonizing microRNA regulation for therapeutic and experimental applications. Nat. Rev. Genet. 2009; 10:578–585. [PubMed: 19609263]
 12. Brown BD, Venneri MA, Zingale A, Sergi L, Naldini L. Endogenous microRNA regulation suppresses transgene expression in hematopoietic lineages and enables stable gene transfer. Nat. Med. 2006; 12:585–591. [PubMed: 16633348]
 13. Bennett D, Sakurai F, Shimizu K, Matsui H, Tomita K, Suzuki T, Katayama K, Kawabata K, Mizuguchi H. Further reduction in adenovirus vector-mediated liver transduction without largely affecting transgene expression in target organ by exploiting microRNA-mediated regulation and the Cre-loxP recombination system. Mol. Pharmaceutics. 2012; 9:3452–3463.
 14. Wu C, Lin J, Hong M, Choudhury Y, Balani P, Leung D, Dang LH, Zhao Y, Zeng J, Wang S. Combinatorial control of suicide gene expression by tissue-specific promoter and microRNA regulation for cancer therapy. Mol. Ther. 2009; 17:2058–2066. [PubMed: 19809402]
 15. Luo Y, Zhu D. Combinatorial control of transgene expression by hypoxia-responsive promoter and microRNA regulation for neural stem cell-based cancer therapy. Biomed. Res. Int. 2014; 2014:751397. [PubMed: 24864258]
 16. Colin A, Faideau M, Dufour N, Auregan G, Hassig R, Andrieu T, Brouillet E, Hantraye P, Bonvento G, Deglon N. Engineered lentiviral vector targeting astrocytes *in vivo*. Glia. 2009; 57:667–679. [PubMed: 18942755]
 17. Karali M, Manfredi A, Puppo A, Marrocco E, Gargiulo A, Allocca M, Corte MD, Rossi S, Giunti M, Bacci ML, Simonelli F, Surace EM, Banfi S, Auricchio A. MicroRNA-restricted transgene expression in the retina. PLoS One. 2011; 6:e22166. [PubMed: 21818300]
 18. He M, Liu Y, Wang X, Zhang MQ, Hannon GJ, Huang ZJ. Cell-type-based analysis of microRNA profiles in the mouse brain. Neuron. 2012; 73:35–48. [PubMed: 22243745]
 19. Rasmussen M, Kong L, Zhang GR, Liu M, Wang X, Szabo G, Curthoys NP, Geller AI. Glutamatergic or GABAergic neuron-specific, long-term expression in neocortical neurons from helper virus-free HSV-1 vectors containing the phosphate-activated glutaminase, vesicular glutamate transporter-1, or glutamic acid decarboxylase promoter. Brain Res. 2007; 1144:19–32. [PubMed: 17331479]
 20. Ottersen OP, Storm-Mathisen J. Glutamate- and GABA-containing neurons in the mouse and rat brain, as demonstrated with a new immunocytochemical technique. J. Comp. Neurol. 1984; 229:374–392. [PubMed: 6150049]
 21. Tan CL, Plotkin JL, Veno MT, von Schimmelmann M, Feinberg P, Mann S, Handler A, Kjems J, Surmeier DJ, O'Carroll D, Greengard P, Schaefer A. MicroRNA-128 governs neuronal excitability and motor behavior in mice. Science. 2013; 342:1254–1258. [PubMed: 24311694]
 22. Kozomara A, Hunt S, Ninova M, Griffiths-Jones S, Ronshaugen M. Target repression induced by endogenous microRNAs: large differences, small effects. PLoS One. 2014; 9:e104286. [PubMed: 25141277]

23. Hu HY, Guo S, Xi J, Yan Z, Fu N, Zhang X, Menzel C, Liang H, Yang H, Zhao M, Zeng R, Chen W, Paabo S, Khaitovich P. MicroRNA expression and regulation in human, chimpanzee, and macaque brains. *PLoS Genet.* 2011; 7:e1002327. [PubMed: 22022286]
24. Lattanzi A, Gentner B, Corno D, Di Tomaso T, Mestdagh P, Speleman F, Naldini L, Gritti A. Dynamic activity of miR-125b and miR-93 during murine neural stem cell differentiation and in the subventricular zone neurogenic niche. *PLoS One.* 2013; 8:e67411. [PubMed: 23826292]
25. Ramirez S, Liu X, Lin PA, Suh J, Pignatelli M, Redondo RL, Ryan TJ, Tonegawa S. Creating a false memory in the hippocampus. *Science.* 2013; 341:387–391. [PubMed: 23888038]
26. Kawashima T, Kitamura K, Suzuki K, Nonaka M, Kamijo S, Takemoto-Kimura S, Kano M, Okuno H, Ohki K, Bito H. Functional labeling of neurons and their projections using the synthetic activity-dependent promoter E-SARE. *Nat. Methods.* 2013; 10:889–895. [PubMed: 23852453]
27. Amendola M, Giustacchini A, Gentner B, Naldini L. A double-switch vector system positively regulates transgene expression by endogenous microRNA expression (miR-ON vector). *Mol. Ther.* 2013; 21:934–946. [PubMed: 23439497]
28. Bloom RJ, Winkler SM, Smolke CD. A quantitative framework for the forward design of synthetic miRNA circuits. *Nat. Methods.* 2014; 11:1147–1153. [PubMed: 25218181]
29. Han X. *In vivo* application of optogenetics for neural circuit analysis. *ACS Chem. Neurosci.* 2012; 3:577–584. [PubMed: 22896801]
30. Fenno LE, Mattis J, Ramakrishnan C, Hyun M, Lee SY, He M, Tucciarone J, Selimbeyoglu A, Berndt A, Grosenick L, Zalocusky KA, Bernstein H, Swanson H, Perry C, Diester I, Boyce FM, Bass CE, Neve R, Huang ZJ, Deisseroth K. Targeting cells with single vectors using multiple-feature Boolean logic. *Nat. Methods.* 2014; 11:763–772. [PubMed: 24908100]
31. Ekstrand MI, Nectow AR, Knight ZA, Latcha KN, Pomeranz LE, Friedman JM. Molecular profiling of neurons based on connectivity. *Cell.* 2014; 157:1230–1242. [PubMed: 24855954]
32. Harraz MM, Dawson TM, Dawson VL. MicroRNAs in Parkinson's disease. *J. Chem. Neuroanat.* 2011; 42:127–130. [PubMed: 21295133]
33. Xu B, Hsu PK, Stark KL, Karayiorgou M, Gogos JA. Derepression of a neuronal inhibitor due to miRNA dysregulation in a schizophrenia-related microdeletion. *Cell.* 2013; 152:262–275. [PubMed: 23332760]
34. Han X, Qian X, Bernstein JG, Zhou HH, Franzesi GT, Stern P, Bronson RT, Graybiel AM, Desimone R, Boyden ES. Millisecond-timescale optical control of neural dynamics in the nonhuman primate brain. *Neuron.* 2009; 62:191–198. [PubMed: 19409264]

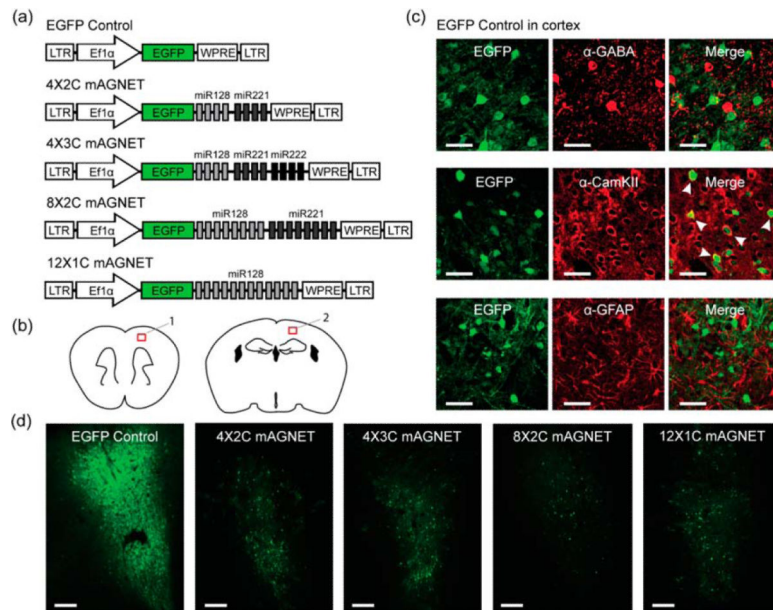


Figure 1. mAGNET design and experimental setup (a) EGFP control and mAGNET lentiviral construct designs with miRNA recognition sites, long terminal repeats (LTR) and the woodchuck hepatitis virus posttranscriptional regulatory element (WPRE). (b) Cortical injection sites in the mouse brain—motor cortex. (1) +1.000 mm ML, +1.800 mm AP, -1.250 mm DV, parietal cortex. (2) +1.000 mm ML, -1.500 mm AP, -0.900 mm DV. (c) Representative confocal images of EGFP fluorescence from cortical cells expressing the EGFP control, α -GABA, α -CAMKII, or α -GFAP immunofluorescence, and colocalization. Scale bars 40 μ m. Arrowheads indicate examples of EGFP colocalization with immunofluorescence. (d) Comparison of viral transduction at motor cortex (1) sites across mice infected with the EGFP control or one of the mAGNET constructs. Scale bars 150 μ m.

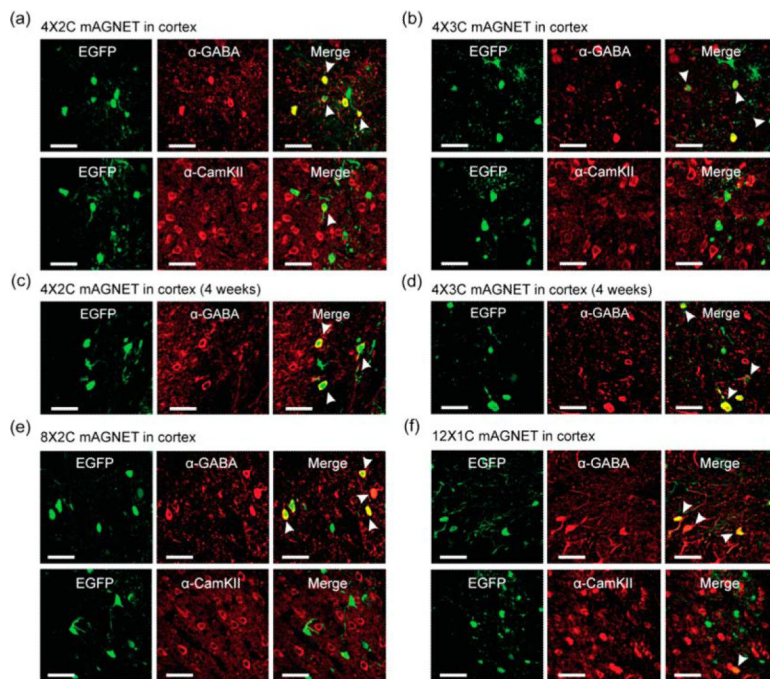


Figure 2. mAGNETs preferentially target cortical inhibitory neurons. Representative confocal images from cortical injection sites, of EGFP fluorescence from cells expressing the 4X2C (a,c), 4X3C (b,d), 8X2C (e), or 12X1C (f) mAGNET, α -GABA and/or α -CAMKII immunofluorescence, and colocalization. Scale bars: 40 μ m. Arrowheads indicate examples of EGFP colocalization with immunofluorescence. (c,d) Mice sacrificed and immunohistochemistry performed at 4 weeks postinjection; all other immunohistochemistry performed at 2 weeks postinjection.

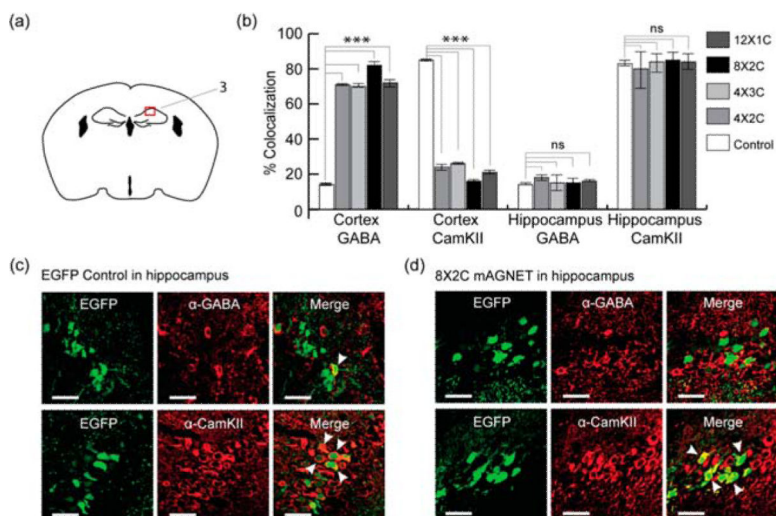


Figure 3. mAGNET targeting is brain-region specific. (a) Hippocampal injection site in the mouse brain–hippocampus (3) +1.000 mm ML, –1.500 mm AP, –1.750 mm DV. (b) Quantification of EGFP fluorescence colocalization with α -GABA or α -CamKII immunofluorescence at 2 weeks postinjection ($n = 2$ mice each design). Cortex data is pooled across both cortical injection sites. *** $p < 0.0005$, or ns (no significance) Pearson's chi squared test (see Supporting Information). (c,d) Representative confocal images from hippocampal injection site of EGFP fluorescence from cells expressing the EGFP control (c) or 8X2C mAGNET (d), α -GABA and α -CAMKII immunofluorescence, and colocalization. Scale bars: 40 μ m. Arrowheads indicate examples of EGFP colocalization with immunofluorescence.

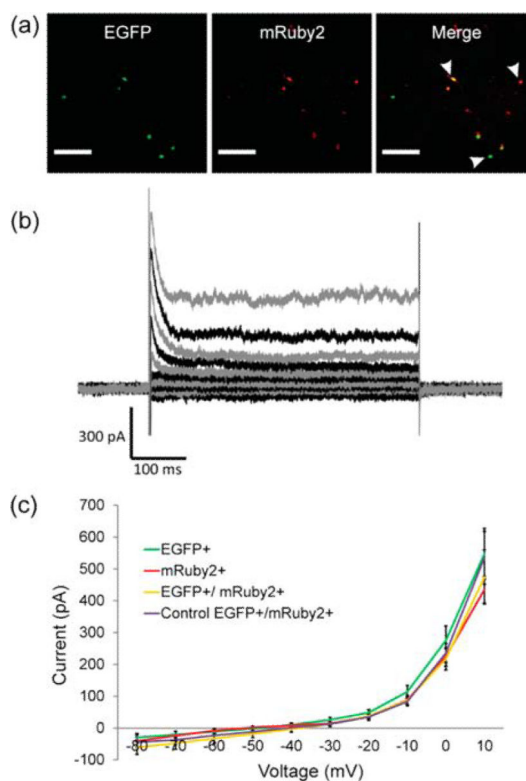


Figure 4. mAGNET regulation is not associated with electrophysiological changes. (a) Representative image showing mAGNET-transfected neurons expressing only EGFP (EGFP+), only mRuby2 (mRuby2+) or both EGFP and mRuby2 (EGFP+/mRuby2+). White arrows indicate exemplar cells of these three types. Scale bars 100 μm . (b) Representative voltage traces for a EGFP+/mRuby2+ mAGNET-transfected neuron, clamped at -80 to 10 mV (bottom to top) at 10 mV intervals. (c) Mean whole-cell currents recorded in voltage clamp mode were plotted *versus* voltage. Error bars show mean \pm standard error of mean ($n = 6-8$ neurons for each group). Note there are no significant electrophysiological differences.

Table 1mAGNET Inhibitory Neuron Target Selectivity Across Brain Areas^a

injection site	marker	control	4X2C	4X3C	8X2C	12X1C
cortex (1)	α -GABA	14% (123)	70% ^{***} (53)	69% ^{***} (68)	83% ^{***} (112)	72% ^{***} (104)
	α -CamKII	86% (144)	24% ^{***} (97)	23% ^{***} (90)	15% ^{***} (117)	23% ^{***} (103)
cortex (2)	α -GABA	13% (105)	72% ^{***} (87)	72% ^{***} (53)	80% ^{***} (54)	73% ^{***} (55)
	α -CamKII	85% (110)	24% ^{***} (62)	31% ^{***} (55)	16% ^{***} (55)	17% ^{***} (63)
hippocampus (3)	α -GABA	14% (121)	18% (71)	15% (103)	15% (120)	16% (76)
	α -CamKII	83% (107)	80% (66)	84% (73)	85% (119)	84% (58)

^aPercentages of GFP+ cells colocalized with α -GABA or α -CamKII for each construct by injection site; numbers in parentheses indicate the number of GFP+ cells analyzed.

^{***} $p < 0.0005$ Pearson's chi squared test (see Supporting Information). $N = 2$ mice tested for each condition.

Author Manuscript

Author Manuscript

Author Manuscript

Author Manuscript